JMBFS
Journal of Microbiology, Biotechnology and Food Sciences
International peer-reviewed scientific online journal
Published by Faculty of Biotechnology and Food Sciences

THE ANTI-*ASPERGILLUS* POTENTIAL OF OPTIMIZED BIOSYNTHESIZED REDUCED GRAPHENE OXIDE/SILVER NANOCOMPOSITE USING *ESCHERICHIA COLI* D8 (MF062579)

Mohamed M. El-Zahed, Zakaria A. M. Baka, Ahmed K.A. El-Sayed, Mohamed. I. Abou-Dobara*

Address(es): Mohamed M. El-Zahed, PhD.
Damietta University, Faculty of Science, Department of Botany and Microbiology, New Damietta, Egypt.

*Corresponding author: mohamed.marzouq91@du.edu.eg

https://doi.org/10.55251/jmbfs.5864

ARTICLE INFO

Received 22. 2. 2022
Revised 7. 7. 2022
Accepted 2. 8. 2022
Published 1. 10. 2022

Regular article

OPEN ACCESS

ABSTRACT

Conventional antifungal agents have failed to treat several infectious diseases of many *Aspergillus* strains. These strains have been linked to the production of high-potency mycotoxins, which cause mould diseases on fruits and vegetables and have negative health consequences. The current study aimed to develop new effective nanomaterials using efficient methods that were stable and antifungal. The current work has been carried out to use the free cell supernatant of *Escherichia coli* D8 (MF062579) in the biosynthesis of reduced graphene oxide/silver nanocomposite (rGO/AgNC). At room temperature, the nanocomposite was prepared by an economical and simple one-step approach. Different parameters were optimized in the biofabrication of rGO/AgNC such as silver nitrate concentration, bacterial supernatant concentration, pH value, and temperature. Ultraviolet-visible spectroscopy (UV-Vis), Fourier transform infrared spectroscopy (FT-IR), transmission electron microscopy (TEM), X-ray diffraction (XRD), and Zeta analyses were used to evaluate the optimized rGO/AgNC. The biosynthesis process was performed within minutes in the incidence of solar irradiation. The mean size of silver nanoparticles (AgNPs) was estimated to be 9-18 nm. The biogenesis of spherical-shaped, well-dispersed AgNPs was validated by TEM images. AgNPs have a positive potential value, as seen by the zeta potential graph. rGO/AgNC had a harmful effect on the ultrastructure of rGO/AgNC-treated *Aspergillus* including membranes damage, malformation, and complete lysis of fungal cells in addition to enzymatic inhibition in lactate dehydrogenase activity. This study states a well-designed approach to develop a new antimicrobial agent, rGO/AgNC, against pathogenic human and phytopathogenic *Aspergillus* spp. in addition to a probable mechanism for the nanomaterial's antimicrobial action.

Keywords: *Antifungal*, *Aspergillus*, *Escherichia coli*, silver, nanocomposite, reduced graphene oxide

INTRODUCTION

Recently, nanobiotechnology has developed as a technology that is cutting edge multidisciplinary involving chemistry, physics, and biology **(Boisselier and Astruc 2009; Kafshgari *et al.* 2015; Hassoun *et al.* 2022)**. Nanobiotechnology employs biosystems for example plant extracts, fungus, bacteria, and virus to synthesize economical, safe, and environmentally friendly nanoparticles (NPs) **(Ahmad *et al.* 2005; Kakoti *et al.* 2022)**. Physicochemical, electrical, magnetic, and biological characteristics of nanomaterials with diameters ranging from 1 to100 nm alter dramatically when compared to materials with larger scales **(Morais *et al.* 2014)**.

Bacteria are the most unique microorganisms in the extracellular biosynthesis of nanomaterials owing to their rapid growth, high efficiency, and ease of use when compared to other microorganisms and plants **(Abbaszadegan *et al.* 2015)**. In contrast to intracellular biosynthesis, extracellular biosynthesis has lately gained popularity because of its simplicity and reduced time requirements with no further downstream processing **(Balakumaran *et al.* 2016)**. Furthermore, nanomaterials' size and shape could be controlled by manipulating the concentrations of both silver ion and bacterial supernatant, pH value, incubation period, and temperature **(Sathishkumar *et al.* 2010; Krishnaraj *et al.* 2012)**, as well as the presence of solar irradiation **(Boopathi *et al.* 2012)**.

Many researchers reported the extracellular bacterial biosynthesis of silver nanomaterials. *Lactobacillus*, *Escherichia coli*, and *Pseudomonas aeruginosa* have been documented as bionanofactories **(Lengke and Southam 2006)**. *L. garvieae* and *Enterococcus faecium* were found in the biosynthesis of nanosilver **(Sintubin *et al.* 2009)**. Silver (Ag) and silver nanomaterials have potent antimicrobial action against different pathogens **(Baskaran 2013)**. However, nanosilver was reported to be higher efficient than bulk Ag **(El-Dein *et al.* 2021)**, Ag nanomaterials are effective fungicides for *Aspergillus terreus*, *A. niger*, *A. flavus*, *Candida tropicalis*, and *C. albicans* **(Mallmann *et al.* 2015)**. One of the highly harmful fungi is the *Aspergillus* species. Many *Aspergillus* strains could release high vigorous mycotoxins called aflatoxins and ochratoxins that cause mould diseases on vegetables and fruits including apricots, onions, and peanuts **(Abarca *et al.* 1994)**. The presented work aimed to biosynthesize and optimize reduced graphene oxide/silver nanocomposite (rGO/AgNC) and study its antimycotic action against *A. flavus*, *A. fumigatus*, and *A. niger*.

MATERIALS AND METHODS

Microbial strains

E. coli D8 (accession number: MF062579) and fungal strains (*A. flavus* Link ex Fries group, *A. fumigatus* Fresenius, and *A. niger* van Tiegh) were attained from the Microbiology Laboratory, Faculty of Science, Damietta University. Strains were conserved at -20°C in a yeast extract peptone glycerol medium (YPG), and re-established in potato dextrose agar (PDA, Becton Dickinson, Mexico) plates (48 to 72 h at 30°C).

Extracellular biosynthesis of rGO/AgNC

E. coli D8 was cultivated aerobically in a nutrient broth medium (Oxoid), for 24 hr at 37°C and 150 rpm. The bacterial growth was centrifuged at 5000 rpm for 15 min under aseptic conditions to collect culture supernatant and then passed through millipore filters. In 100ml of distilled water, 0.3 g of graphene oxide (GO) powder (Sigma Aldrich, purity 99.99%) was ultrasonicated for 2 hr. An aqueous solution of 1 mM silver nitrate ($AgNO_3$, Panreac Quimica S.L.U, Barcelona, Spain) was treated with free cell supernatant and GO colloidal solution (1:1:1 v/v) in a 250ml conical flask. $AgNO_3$, GO and nutrient broth mixture (1:1:1 v/v) was prepared and utilised as a blank. The flasks were well-shaken and kept in sunlight at room temperature. Similarly, the biosynthesis of rGO/AgNC in dark conditions was tested and observed via the visible colour alteration of the mixture into brown colour. The reaction mixture absorbance of (3 ml aliquots) was examined by an Ultraviolet-visible (UV-Vis) spectrophotometer (Beckman DU-40) **(Shahverdi *et al.* 2007)**.

Optimization of the extracellular biosynthesized rGO/AgNC

Different concentrations of $AgNO_3$ solutions (1, 2, 3, 4, 5, and 6 mM) were evaluated to select the best concentration for the synthesis of rGO/AgNC at pH 7±0.2 at room temperature, dark conditions and 150 rpm for 5 days (Mishra *et al.* 2014). Different concentrations of bacterial supernatant (1, 10, 20, 30, 40 and, 50%) were prepared and then added to $AgNO_3$ solutions to enhance the synthesis of rGO/AgNC. Different temperatures (20-50°C) and pH values (1-10) were also

tested. The biosynthesis of rGO/AgNC was detected in sunlight during various time (1-6 min) intervals of incubation **(Boopathi *et al*. 2012)**.

Description of the biosynthesized rGO/AgNC

The fabrication of rGO/AgNC was monitored by UV-Vis spectroscopy; Beckman DU-40. Fourier transform infrared spectroscopy (FT-IR) of rGO/AgNC was analysed using FT/IR-4100typeA. The rGO/AgNC X-ray diffraction patterns (XRD) were also recorded with an X-ray diffractometer (model LabX XRD-6000, Shimadzu, Japan) at 40 kV and 30mA. Transmission electron microscopic (TEM) analysis was done according to **Wang (2000)** using TEM apparatus (200 kV, TEM JEOL JEM-2100, Japan). Zeta potential analyser measured size distribution by volume, surface charge, and stability of AgNPs and nanocomposite **(Ruud *et al*. 1976; Hanaor *et al*. 2012)**.

Stability of the biosynthesized rGO/AgNC

The stability of rGO/AgNC was tested according to El-Zahed et al. (2021) by dissolving rGO/AgNC in different solvents (hexane, toluene, acetone, n-butyl alcohol, dimethylformamide (DMF), ethanol, methanol, and water) and detecting its Zeta average size (Zavg) and polydispersity index (PDI) by Malvern Zetasizer Nano-ZS90, Malvern, UK.

The anti-*Aspergillus* activity of the biosynthesized rGO/AgNC

The spore suspension of inoculums (0.08 to 1 × 10^5 CFU/ml) was prepared according to the method designated by **Espinel-Ingroff *et al.* (2007)**.

Agar well diffusion method

The fungicidal action of rGO/AgNC against three *Aspergillus* strains (*A. flavus*, *A. fumigatus*, and *A. niger*) was demonstrated using *in vitro* agar well diffusion test according to the guidelines of the Clinical and Laboratory Standards Institute (Clinical and Laboratory Standards, 2006). 100 µl of different concentrations (50, 100 and 150µg/ml) of GO, rGO/AgNC, $AgNO_3$, and miconazole (Sigma-Aldrich, as standard antifungal) were prepared in dimethyl sulfoxide (DMSO) and added separately under aseptic conditions into 5mm wells in Sabouraud dextrose agar (SDA, Becton Dickinson, Mexico) plates prior to incubation at 30°C for 5 days. The inhibition zones were calculated in millimetres (mm). The assays were performed three times and the findings were expressed as means.

Radial mycelial growth inhibition

The inhibition of fungal radial growth was investigated according to Quiroga *et al*. (2004). Briefly, a 5 mm disc of 7-days culture was cut and placed upside down in the centre of SDA plates amended with 200 µL of the tested antifungal agents (150µg/ml); GO, $AgNO_3$, rGO/AgNC, and miconazole. Inoculated SDA plates without antifungal agents were used as a control. Three replicates for each examined fungus were utilised, and the plates were incubated at 30°C for 7 days. The average diameter of the growth was measured in mm and percent inhibition rates were calculated through the following formula:

$$\text{Inhibition rate (\%)} \frac{R - r}{R}$$

Where, R represents the fungal radial growth on the control, while r represents the fungal radial growth on the treated plate.

Ultrastructure study

The exponential-phase culture of *A. niger* (as a model for fungi) treated with rGO/AgNC (150µg/ml) was taken, prepared, and examined using TEM at Mansoura University.

L-lactate dehydrogenase

Total protein content of untreated and rGO/AgNC-treated fungi was estimated by the Bradford dye-binding method (Bradford 1976). L-lactate dehydrogenase (LDH) activity was measured spectrophotometrically depending on the presence of L-lactate and NAD^+ reduction. The enzyme (0.1-10 units per millilitre) was dissolved just before assay in 0.5 M phosphate buffer, pH 7.0. Use per millilitre of reaction mixture: 0.8 ml of 0.5 M phosphate buffer; 0.05 ml of NAD^+; 0.1 mL of sodium lactate; 5-50 µl of enzyme solution, and water to make the correct final volume (3.0 ml). The increase of absorbance at 340 nm was recorded at 25°C, and the maximal (initial) rate was used for calculations. One unit of enzyme activity reduces NAD^+ at the rate of 1 µmole per minute at 25°C. The units of enzyme per millilitre of the mixture are calculated from the absorbance change rate (Yoshida and Freese, 1975).
The units of LDH enzymes in the reaction mixture are obtained from the initial rate of diminution of absorbance at 340 nm using the following equation:

$$\text{Units of enzyme } (\mu U/mL) = \frac{O.D}{T} \times \frac{Vt}{6.22} \times \frac{1}{Vu} \times 1000$$

Where, O.D resemble the optical density at 340 nm, Vt is the total reaction volume, T is the time in minutes, 6.22 $mM^{-1}cm^{-1}$ is the molar extinction coefficient of NADH, 1000 is the conversion factor from a unit of the enzyme into µU and Vu is the volume of enzyme solution used for the assay.
Specific activity is expressed as the number of enzyme units per microgram of protein.

Statistical analysis

The results were analysed with ANOVA using SPSS software version 18. The significant level was set at $p<0.05$. The experiments were done in triplicate. All values were expressed as the mean±standard deviation (SD) (O'connor 2000).

RESULTS

The results showed that *E. coli* D8 could be used to biosynthesize rGO/AgNC in dark conditions within 72 hr. The first indication of the nanocomposite production was the colour change into brown. rGO/AgNC showed a peak at 425 nm (Figure 1).

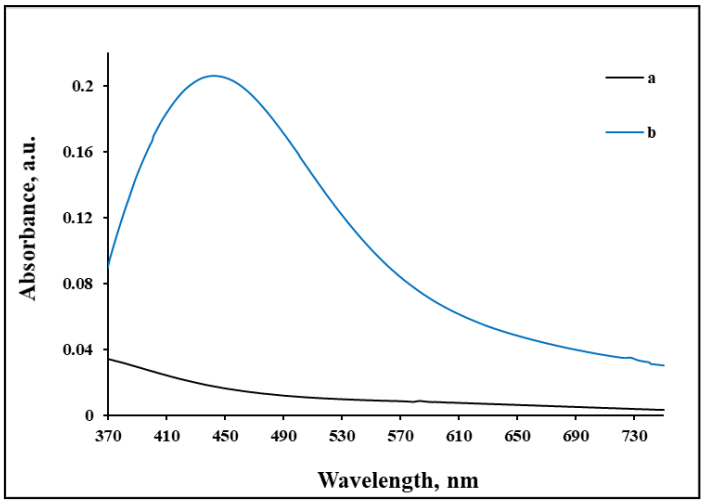

Figure 1 Ultraviolet-visible spectroscopy of GO; (a) and biosynthesized rGO/AgNC by *E. coli* D8; (b).

Optimization of *E. coli* D8 biosynthesized rGO/AgNC

All UV-Vis spectra of the experimented concentrations of $AgNO_3$ (1-6 mM) sustained the nanocomposite production (Figure 2A). Among the concentrations tested, 3 mM greatly enhanced the rGO/AgNC biosynthesis. Also, among the concentrations of bacterial supernatant tested, 40% (v/v %) appeared to be the best for the biosynthesis of rGO/AgNC (Figure 2B), whereas other tested bacterial supernatant concentrations did not favour the biosynthesis. Based on colour change, pH 4 and 10 resulted in NPs aggregation. On the other hand, colour did not change at pH (1-3) and a very small colour change was observed at pH values of 4-6. The brown colour development initiated at pH5 and 6 and the intensity of the brown colour raised with the rise in pH value (Figure 2C). Amongst various levels of temperature, it was found that 30°C was the optimal temperature for rGO/AgNC biosynthesis and supernatant below or above this temperature, rGO/AgNC production decreased gradually (Figure 2D). The biosynthesis of rGO/AgNC at sunlight started in the first minute (Figure 2E).

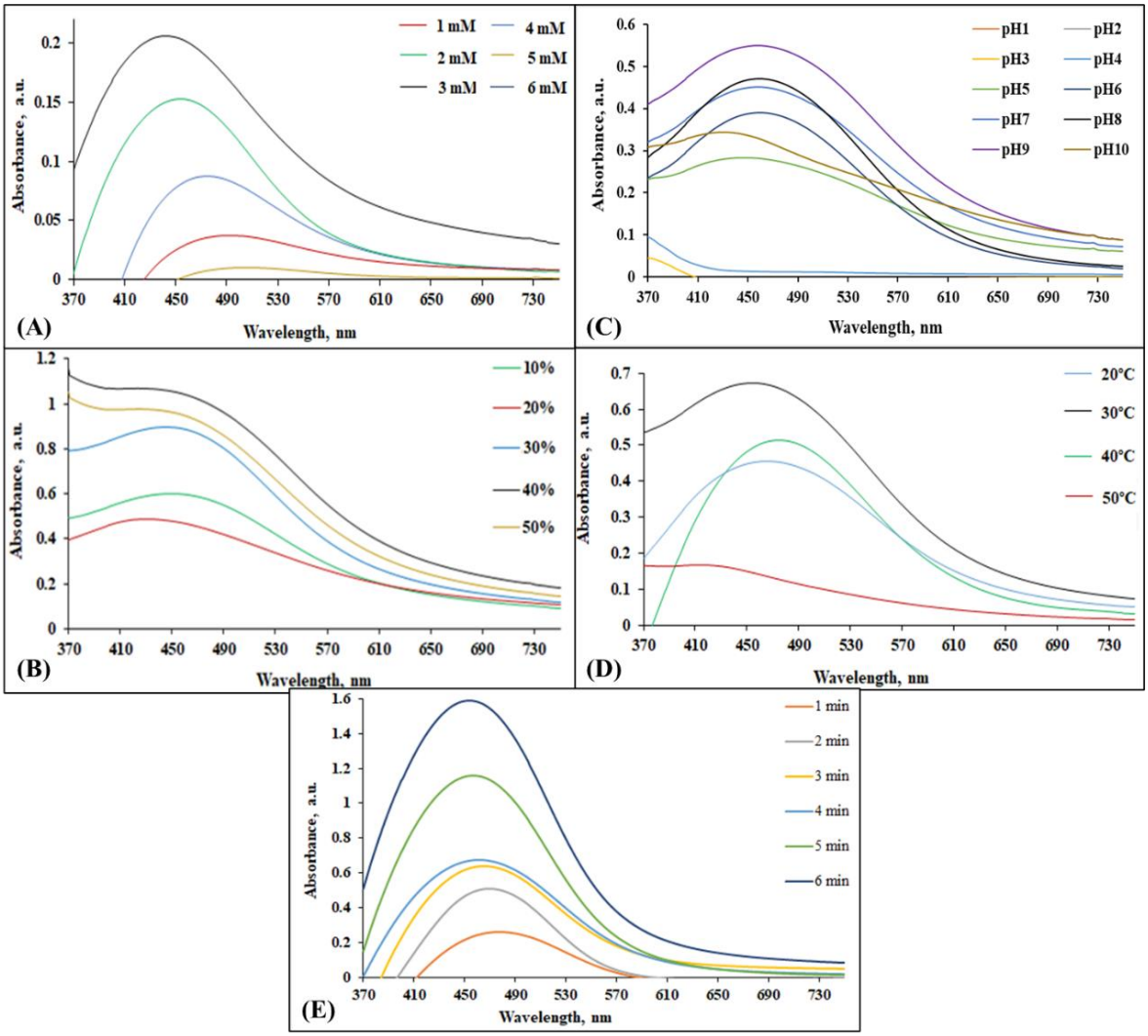

Figure 2 Optimization of rGO/AgNC biosynthesis. (A) Concentrations of $AgNO_3$. (B) Concentrations of bacterial supernatant. (C) pH. (D) Temperature. (E) Time exposure to solar irradiation.

Characterization of optimized rGO/AgNC

The optimized biosynthesized rGO/AgNC by *E. coli* D8 was assessed by UV-Vis spectrophotometer, FT-IR and XRD spectra, TEM, Zeta potential analyser and size distribution by volume. The brown colour formed in the optimized medium proved the biosynthesis of AgNPs with an adsorption peak of 443 nm.

The FT-IR spectrum (Figure 3) of GO revealed an adsorption peak at 3436.53 cm^{-1} which is assigned to OH stretching. It showed peaks at 1729.83, 1644.02, 1379.82, and 1035.59 cm^{-1}, which are attributed to the C = O stretching vibration of COOH groups, C=O, C–OH, and C–O vibrations from alkoxy groups, respectively. After reduction using *E. coli* D8 supernatant, the intensity of these peaks was considerably reduced, representing that the number of oxygen-containing groups of GO decreased dramatically **(Zheng *et al*. 2013)**.

Figure 3B displays the XRD patterns of GO and rGO/AgNC in which GO shows a notable peak at 11.6° resembling plane GO (002) and interplanar space at 0.79 Å, refers to its oxidation state **(Li and Liu 2010)**. In rGO/AgNC XRD, the disappearance of the peak at 11.6° and the appearance of the broad peak at 23.9°indicated to the complete reduction of GO to rGO by *E. coli* D8 supernatant. The XRD of rGO/AgNC showed diffraction peaks of AgNPs at 37.8°, 44.5°, 65.4°, and 78.15°, resembling the face concentrated cubic (fcc) of AgNPs planes (111), (200), (220) and (311), respectively. The strong diffraction peak at 37.8° was attributed to crystalline Ag, confirming the fabrication of Ag crystals with high purity in rGO/AgNC **(Das *et al*. 2011)**.

The size distribution by volume confirmed the good dispersion of these particles (Figure 3C) and the Zeta potential of the nanocolloidal solution was +24.1mV (Figure 3D). TEM scans revealed AgNPs that were spherical and evenly distributed (Figures 3E and F). The average size of the AgNPs was 13.2 nm, with a standard variation of 0.25 nm.

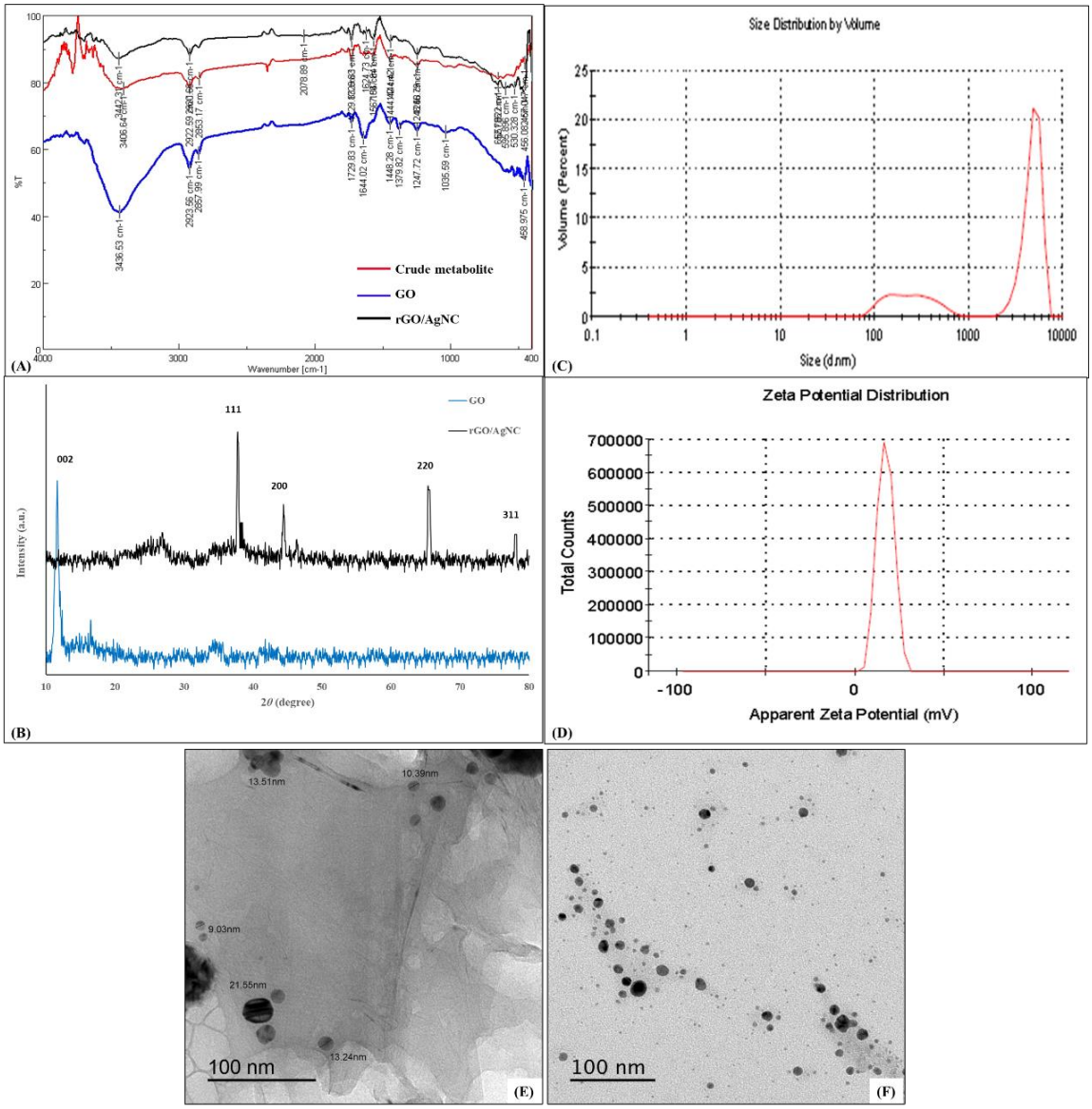

Figure 3 Characterization of the biosynthesized rGO/AgNC. (A) FT-IR. (B) XRD. (C) The size distribution by volume. (D) Zeta analysis. (E) and (F) TEM. Bars scale = 100 nm (E and F).

Stability of the biosynthesized rGO/AgNC

The prepared nanocomposite was stable in all solvents for more than 3 h. Table 1 indicated the good dispersion of rGO/AgNC in polar solvents such as DMF and ethanol whereas it was weak in nonpolar solvents.

Table 1 The Zavg and PDI for the rGO/AgNC in different solvents.

Solvent	Zavg (nm)	PDI (d.nm)
Hexane	631	0.544
Toluene	1157	0.863
Acetone	1599	0.785
n-butanol	340	0.487
DMF	386	0.459
Ethanol	477	0.756
Methanol	854	0.812
Water	301	0.400

The anti-*Aspergillus* activity of rGO/AgNC

The biosynthesized rGO/AgNC using *E. coli* D8 showed good antifungal activity against all tested *Aspergillus* strains as shown in Table 2.

Table 2 Antifungal activity of rGO/AgNC in comparison with other antifungal agents

Ligands	Concentration, µg/ml	Inhibition zone (mean±SE, n=3, mm)		
		A. flavus **Link ex Fries group**	***A. fumigatus*** **Fresenius**	***A. niger*** **van Tiegh**
GO	50	-ve	-ve	-ve
	100	-ve	-ve	-ve
	150	-ve	-ve	-ve
$AgNO_3$	50	6 ± 0.14	7 ± 0.06	12 ± 0.14
	100	9 ± 0.06	10 ± 0.06	14 ± 0.06
	150	12 ± 0.03	12 ± 0.03	19 ± 0.03
rGO/AgNC	50	13 ± 0.03	12 ± 0.06	15 ± 0.06
	100	15 ± 0.03	14 ± 0.03	18 ± 0.06
	150	19 ± 0.03	18 ± 0.03	23 ± 0.03
Miconazole	50	3 ± 0.14	6 ± 0.06	11 ± 0.03
	100	7 ± 0.03	9 ± 0.06	13 ± 0.03
	150	10 ± 0.06	11 ± 0.03	18 ± 0.03

Figure 4 and Figure 5 show the mycelium radial growth and the inhibition of fungal growth with and without treatment with tested antifungal agents, respectively. rGO/AgNC showed good antifungal action against *A. niger* (83%) and moderate efficacy against *A. flavus* (68%) and *A. fumigatus* (63%).

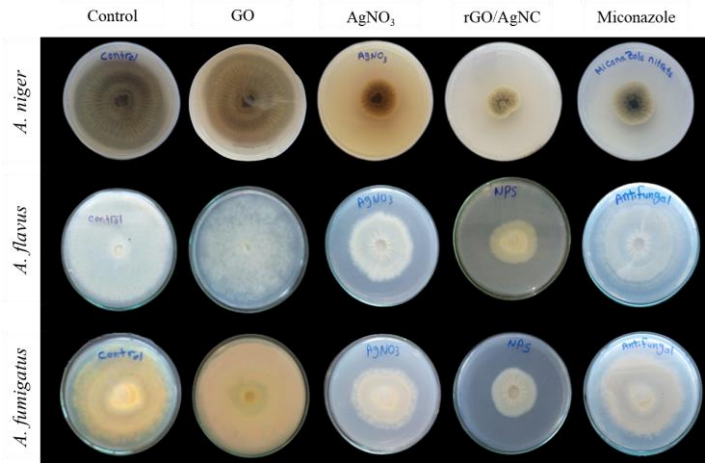

Figure 4 Antifungal activity of GO, $AgNO_3$, rGO/AgNC, and miconazole against *Aspergillus* strains at a concentration of 150µg/ml.

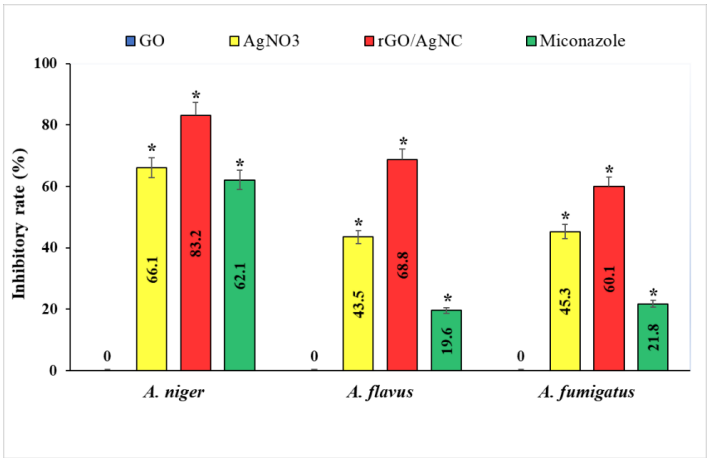

Figure 5 Inhibitory rate percent of GO, $AgNO_3$, rGO/AgNC, and miconazole against *Aspergillus* strains at a concentration of 150µg/ml. *Indicates significant inhibitory rate (p<0.05).

The ultrastructure of rGO/AgNC-treated *A. niger*

TEM micrographs of treated *A. niger* cells showed several ultrastructural changes in comparison to the untreated ones (Figure 6). Treated *A. niger* had reduced size, lipid globules, and large vacuole with a harsh trickle of cytoplasmic contents. In addition, the plasma membrane was separated from the fungal cell. These results confirmed the damaging effect of rGO/AgNC on the *A. niger* cells due to the interactions of AgNPs with the cellular component.

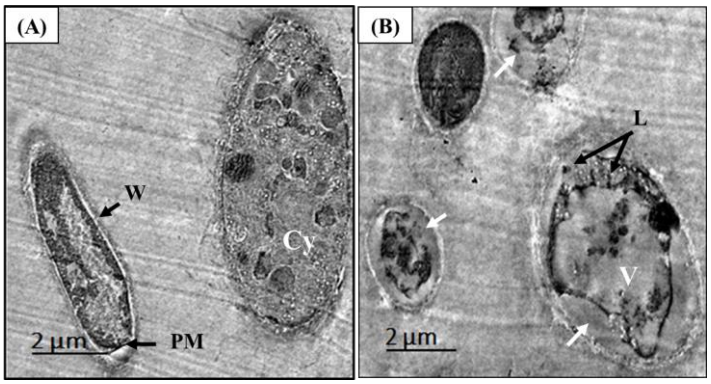

Figure 6 The antifungal activity of rGO/AgNC on the ultrastructure of *A. niger*. (A) Control without rGO/AgNC treatment. W is the cell wall, PM is the plasma membrane, V is the vacuole, and Cy the is compact cytoplasm. (B) Treated sample, note the formation of the large vacuole (V), the space formed between the plasma membrane and cell wall (white arrows), and lipid droplets (L).

LDH activity test

The effects of rGO/AgNC on LDH activity of *A. flavus*, *A. fumigatus*, and *A. niger* are shown in Figure 7 and Table 3. During the assay of LDH activity in the control (without rGO/AgNC) and rGO/AgNC-treated fungi, it was found that the enzymatic activities and specific activities decreased upon treatment.

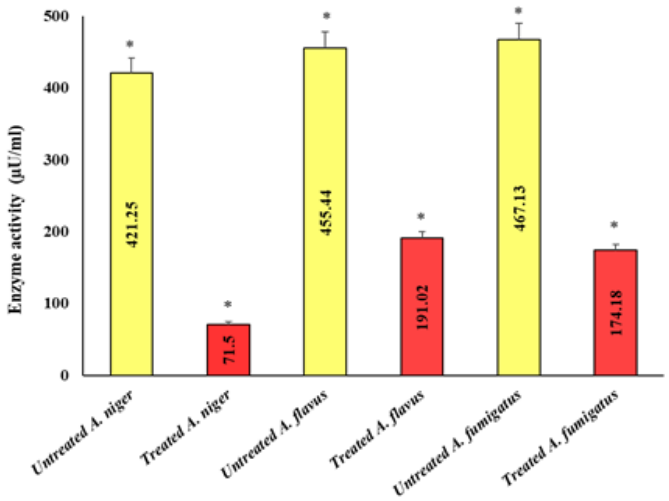

Figure 7 The enzymatic activities of LDH in untreated and rGO/AgNC-treated fungi. *Indicates significant inhibitory rate (p<0.05).

Table 3 Enzymatic activities and specific activities of LDH in untreated and rGO/AgNC-treated fungal strains (mean ± SD).

Fungal strain	Total protein concentration (µg/ml)	Units of the enzyme (µU/ml)	Specific activity (µU/µg)
Untreated *A. niger*	2820 ± 0.03	421.2 ± 0.03	0.149 ± 0.03
Treated *A. niger*	2764 ± 0.03	71.5 ± 0.03	0.026 ± 0.03
Untreated *A. flavus*	2247 ± 0.03	455.44 ± 0.03	0.203 ± 0.03
Treated *A. flavus*	2244 ± 0.03	191.02 ± 0.03	0.085 ± 0.03
Untreated *A. fumigatus*	2645 ± 0.03	467.13 ± 0.03	0.177 ± 0.03
Treated *A. fumigatus*	2601 ± 0.03	174.18 ± 0.03	0.067 ± 0.03

DISCUSSION

Although the antibacterial actions of rGO and its composites have been commonly studied, their antifungal properties are still less reported. Since fungal infection critically threatens public health. The current study provides a simple one-step method for the fabrication of rGO/AgNC and demonstrates its promising antifungal action. This rGO/AgNC was prepared by the bioreduction of GO and $AgNO_3$ with cell-free supernatant of *E. coli* D8 in the presence of sunlight. *E. coli* strains are known for their ability to produce some quinones such as menaquinone, demethylmenaquinone and ubiquinone that reduced Ag ions into AgNPs in the presence of sunlight **(Sharma *et al*. 2012; Panter *et al*. 2022).**

Various parameters were optimised to control the shape, size, and stability of biosynthesized NPs for effective medical applications, including metal ion concentration, cell-free bacterial supernatant concentration, pH, and temperature **(Sathishkumar *et al*. 2010; Krishnaraj *et al*. 2012) and sunlight (Boopathi *et al*. 2012)**.

The colour change from colourless to brown is due to the innervation of Ag surface plasmon vibrations, which confirm the biosynthesis of rGO/AgNC **(Das et al. 2014; Kalimuthu *et al*. 2008; Okumura *et al*. 2016)**.

Monodispersed and stable rGO/AgNC were formed at pH 8. These results are nearly similar to those obtained from extracellular synthesis by *Allophylus cobbe* (Gurunathan *et al*. 2014), *Alcaligenes faecalis* **(El-Deeb *et al*. 2013)**, and *Serratia marcescens* **(Akilandeswari *et al*. 2014)**. Also, temperature affects NPs formation and stability **(Mishra *et al*. 2014)**. In our study, 30ºC was favoured for rGO/AgNC biosynthesis, which is similar to that reported for nanoparticles biosynthesis using *Vitex pedencularis* **(Adebayo-Tayo and Popoola, 2017)**. The production of rGO/AgNC was achieved within 72 hr. after incubation of 1% (v/v %) of cell-free bacterial supernatant with 1 mM of $AgNO_3$ in dark conditions. This is similar to the production rate using *Bacillus flexus* **(Kaur 2018)**, *Bacillus* strain CS 11 (Das *et al*. 2014), *E. coli* **(Vandana and Archana 2016)**, *B. cereus*, *P. aeruginosa*, *Micrococcus luteus*, *Klebsiella pneumoniae*, *Proteus mirabilis*, and *Staphylococcus aureus* **(Baskaran 2013)**. Sunlight participates in a pointed function in the complete reduction of Ag ions at a rapid rate **(Nam *et al*. 2008)**. The biosynthesis in the current study occurred within a minute in the presence of solar irradiation. **Mokhtari *et al*. (2009)** reported the extracellular biosynthesis of AgNPs by *K. pneumoniae* within a few minutes. In another study, *Streptomyces aegyptia* NEAE 102 was used to biosynthesise AgNPs within one minute **(El-Naggar *et al*. 2014)**. The biosynthesized AgNPs had a size range of 9.03-21.55 nm. **Kulkarni *et al*. (2015)** synthesized AgNPs by *Deinococcus radiodurans* with a mean size of 17 nm and AgNPs with a similar size were also produced by *B. licheniformis* NM120-17 **(Gomaa 2017)**. Even inside the aggregates, NPs were not in direct contact, indicating that the NPs were stabilised by a capping agent

produced directly from bacterial proteins. This stability was tested by assessing the zeta potential of the nanocolloidal solution (+24.1mV). This positive zeta potential value indicates that the particles could strongly bind the negatively charged compounds in the microbial cell wall **(Elbeshehy *et al*. 2015)**.

Recently, the antifungal activity of nanomaterials has impressive attention to researchers due to the continuous development of microbial resistance (Nguyen *et al*. 2022). This study presents a much more effective and fast-acting fungicide against a common fungus, *Aspergillus* sp. **(Abarca *et al*. 1994)**. The biofabricated rGO/AgNC had a superior effective toxic action against *A. niger* with an inhibition rate of 83%. **Hazarika *et al*. (2016)** and Adebayo-Tayo and Popoola (2017) demonstrated that *A. niger* growth was inhibited at a rate of 10% and 10.1%, respectively. AgNPs showed anti-*Aspergillus* activity with a 62-75% fungicidal index **(Thenmozhi *et al*. 2013)**. Against *A. niger*, an inhibition rate measured was 15.6% by **Vandana and Archana (2016)** and 21.6% by Devi and Bhimba (2014). Many researchers documented the antimicrobial properties of Ag particles and AgNPs **(Rathod *et al*. 2012)**. When rGO/AgNC and bulk Ag particles were tested against *A. niger*, shown that rGO/AgNC have a stronger antibacterial impact than bulk Ag particles. The antifungal activity revealed a dramatic conversion from no activity of GO to distinct antifungal growth inhibition of the rGO/AgNC. This result was consistent with the previous study that goes is not resistant to fungi **(Dai *et al*. 2016)**. TEM studies confirmed the potent antifungal action of rGO/AgNC against *A. niger* as a fungal model. The untreated hyphal cells of *A. niger* had a healthy cell wall, cell membrane, cytoplasm, and small vacuole. In contrast, several alterations were detected after the treatment by rGO/AgNC such as the presence of lipid droplets and large vacuoles. **Abdel-Hafez *et al*. (2016)** documented the accumulation of AgNPs in the cytoplasm, cell nucleus and cytoplasmic membrane of AgNPs treated fungi that might be the main factor in the major morphologic alterations. Furthermore, the accumulated NPs could interact with DNA and damage it **(Vahdati and Sadeghi, 2013)**. Moreover, Radzig et al. (2013) recorded the ability of small AgNPs to enter the microbial cell membranes and interact with their proteins and enzymes that block, inactivate them and end by the cell death.

LDH enzyme behaviour was used to study the influence of rGO/AgNC on oxidative stress-induced damage in cell respiration. LDH is regarded as a trustworthy indication of oxidative stress in cells **(Sugimoto *et al*., 2010)**. LDH uses NAD^+ as an electron acceptor to catalyse the reversible oxidation of lactate to pyruvate:

$$\text{Pyruvate} + \text{NADH} + H^+ \rightarrow \text{L-lactate} + NAD^+$$

The LDH activities and specific activities in rGO/AgNC-treated fungi decreased after treatment. *A. niger* was attained to be more susceptible to rGO/AgNC action when compared to *A. flavus* and *A. fumigatus*. LDH activity was still present after the treatment with rGO/AgNC, but it decreased from 455.44, 467.13, and 421.2 to 191.02, 174.18, and 71.5µmol $NADH.min^{-1}$ for *A. flavus*, *A. fumigatus* and *A. niger*, respectively. According to *A. niger*, rGO/AgNC strongly inhibited dehydrogenase activity which also was reported by **Gurunathan et al. (2015)**. Besides, Jaworski et al. (2018) stated a decrease in LDH of *S. aureus*, *E. coli*, *C. albicans*, and *S. epidermidis* membrane integrity after the treatment with rGO/AgNC. **Eymard-Vernain et al. (2018)** recommended the interaction of AgNPs with the biomolecule-bearing carboxyl groups of thiol groups that lead to the blocking and inactivation of enzymes. In short, rGO/AgNC has an excellent antifungal activity with a highly stable structure that could be used in agricultural and industrial applications.

CONCLUSIONS

Reduced graphene oxide/silver nanocomposite was biosynthesized using the cell-free bacterial supernatant of *Escherichia coli* D8 (AC: MF062579). The optimized biosynthesized nanocomposite was highly stable and had higher biocidal activity against the pathogenic fungi, *A. flavus* Link ex Fries group, *A. fumigatus* Fresenius, and *A. niger* van Tiegh with antifungal index in the range of 83-63%. The biosynthesis approach was employed to produce a simple, cost-effective, rapid, and eco-friendly nanomaterial with high stability and large quantities.

REFERENCES

Abarca, M. L., Bragulat, M. R., Castella, G., and Cabanes, F. J. (1994). Ochratoxin A production by strains of *Aspergillus niger* var. niger. Appl Environ Microbiol, 60(7), 2650-2652. https://doi.org/10.1128/aem.60.7.2650-2652.1994

Abbaszadegan, A., Ghahramani, Y., Gholami, A., Hemmateenejad, B., Dorostkar, S., Nabavizadeh, M., and Sharghi, H. (2015). The effect of charge at the surface of silver nanoparticles on antimicrobial activity against gram-positive and gram-negative bacteria: a preliminary study. J Nanomater, 2015: 1-8. https://doi.org/10.1155/2015/720654

Abdel-Hafez, S. I., Nafady, N. A., Abdel-Rahim, I. R., Shaltout, A. M., Daròs, J. A., and Mohamed, M. A. (2016). Assessment of protein silver nanoparticles toxicity against pathogenic *Alternaria solani*. 3 Biotech, 6(2), 1-12. https://doi.org/10.1007/s13205-016-0515-6

Adebayo-Tayo, B. C., and Popoola, A. O. (2017). Biogenic synthesis and antimicrobial activity of silver nanoparticles using exopolysaccharides from lactic acid bacteria. Int J Nano Dimens, 8(1), 61-69. https://dx.doi.org/10.22034/ijnd.2017.24377

Ahmad, A., Senapati, S., Khan, M. I., Kumar, R., and Sastry, M. (2005). Extra-/intracellular biosynthesis of gold nanoparticles by an alkalotolerant fungus, *Trichothecium* sp. J Biomed Nanotech, 1(1), 47-53. https://doi.org/10.1166/jbn.2005.012

Akilandeswari, K., Karpagam, P., and Amutha, K. (2014). Rapid biosynthesis, characterization and antimicrobial effects of silver nanoparticles from microorganism *Serratia marcescens*. Int J Biochem Mol, 2(1), 15-24. http://www.irphouse.com/ijmbb/ijmbbv2n1_02_.pdf

Balakumaran, M. D., Ramachandran, R., Balashanmugam, P., Mukeshkumar, D. J., and Kalaichelvan, P. T. (2016). Mycosynthesis of silver and gold nanoparticles: optimization, characterization and antimicrobial activity against human pathogens. Microbiol Res, 182, 8-20. https://doi.org/10.1016/j.micres.2015.09.009

Baskaran, C., and Ratha-bai, B. (2013). Green Synthesis of silver nanoparticles using *Coleus forskohlii* roots extract and its antimicrobial activity against bacteria and fungus. Int j drug dev, 5, 114-119.

Boisselier, E., and Astruc, D. (2009). Gold nanoparticles in nanomedicine: preparations, imaging, diagnostics, therapies and toxicity. Chem Soc Rev, 38(6), 1759-1782. https://doi.org/10.1039/B806051G

Boopathi, S., Gopinath, S., Boopathi, T., Balamurugan, V., Rajeshkumar, R., and Sundararaman, M. (2012). Characterization and antimicrobial properties of silver and silver oxide nanoparticles synthesized by cell-free extract of a mangrove-associated *Pseudomonas aeruginosa* M6 using two different thermal treatments. Ind Eng Chem Res, 51(17), 5976-5985. https://doi.org/10.1021/ie3001869

Bradford, N. J. A. B. (1976). A rapid and sensitive method for the quantitation microgram quantities of a protein isolated from red cell membranes. Analytical Biochemistry, 72(248), e254. https://doi.org/10.1016/0003-2697(76)90527-3

Chou, K. S., Lu, Y. C., and Lee, H. H. (2005). Effect of alkaline ion on the mechanism and kinetics of chemical reduction of silver. Mater Chem Phys, 94(2-3), 429-433. https://doi.org/10.1016/j.matchemphys.2005.05.029

Clinical and Laboratory Standards Document M2-A9. 2006. Performance standards for antimicrobial disk susceptibility tests: Approved standard- Ninth Edition, Clinical and Laboratory Standards Institute, Wayne, Pennsylvania, USA.

Dai, X., Guo, Q., Zhao, Y., Zhang, P., Zhang, T., Zhang, X., and Li, C. (2016). Functional silver nanoparticles as a benign antimicrobial agent that eradicates antibiotic-resistant bacteria and promotes wound healing. ACS Appl Mater Interfaces, 8(39), 25798-25807. https://doi.org/10.1021/acsami.6b09267

Das, M. R., Sarma, R. K., Saikia, R., Kale, V. S., Shelke, M. V., and Sengupta, P. (2011). Synthesis of silver nanoparticles in an aqueous suspension of graphene oxide sheets and its antimicrobial activity. Colloids Surf B, 83(1), 16-22. https://doi.org/10.1016/j.colsurfb.2010.10.033

Das, V. L., Thomas, R., Varghese, R. T., Soniya, E. V., Mathew, J., and Radhakrishnan, E. K. (2014). Extracellular synthesis of silver nanoparticles by the *Bacillus* strain CS 11 isolated from industrialized area. 3 Biotech, 4(2), 121-126. https://doi.org/10.1007/s13205-013-0130-8

Devi, J. S., and Bhimba, B. V. (2014). Antimicrobial potential of silver nanoparticles synthesized using *Ulva reticulata*. Asian J Pharm Clin Res, 7(2), 82-5.

Elbeshehy, E. K., Elazzazy, A. M., and Aggelis, G. (2015). Silver nanoparticles synthesis mediated by new isolates of *Bacillus* spp., nanoparticle characterization and their activity against Bean Yellow Mosaic Virus and human pathogens. Front microbiol, 6, 453. https://doi.org/10.3389/fmicb.2015.00453

El-Deeb B, Mostafa NY, Altalhi A, Gherbawy Y (2013) Extracellular biosynthesis of silver nanoparticles by bacteria *Alcaligenes faecalis* with highly efficient anti-microbial property. Int J Chem Eng 30: 1137-1144.

El-Dein, M. M. N., Baka, Z. A. M., Abou-Dobara, M. I., El-Sayed, A. K. A., and El-Zahed, M. M. (2021). Extracellular biosynthesis, optimization, characterization and antimicrobial potential of *Escherichia coli* D8 silver nanoparticles. JMBFs, 10(4), 648–656. https://doi.org/10.15414/jmbfs.2021.10.4.648-656

El-Naggar, N. E. A., Abdelwahed, N. A., and Darwesh, O. M. (2014). Fabrication of biogenic antimicrobial silver nanoparticles by *Streptomyces aegyptia* NEAE 102 as eco-friendly nanofactory. J Microbiol Biotechnol, 24(4), 453-464. https://doi.org/10.4014/jmb.1310.10095

El-Zahed, M. M., Baka, Z. A., Abou-Dobara, M. I., El-Sayed, A. K., Aboser, M. M., and Hyder, A. (2021). *In vivo* toxicity and antitumor activity of newly green synthesized reduced graphene oxide/silver nanocomposites. Bioresour Bioprocess, 8(1), 1-14. https://doi.org/10.1186/s40643-021-00400-7

Espinel-Ingroff, A., Arthington-Skaggs, B., Iqbal, N., Ellis, D., Pfaller, M. A., Messer, S., ... and Wang, A. (2007). Multicenter evaluation of a new disk agar diffusion method for susceptibility testing of filamentous fungi with voriconazole, posaconazole, itraconazole, amphotericin B, and caspofungin. J Clin Microbiol, 45(6), 1811-1820. https://doi.org/10.1128/JCM.00134-07

Eymard-Vernain, E., Coute, Y., Adrait, A., Rabilloud, T., Sarret, G. and Lelong, C. (2018). The poly-gamma-glutamate of *Bacillus subtilis* interacts specifically with silver nanoparticles. PLoS One 13(5): e0197501. https://doi.org/10.1371/journal.pone.0197501

Garcia, L. S. (Ed.). (2010). Clinical microbiology procedures handbook (Vol. 2). ASM.

Gomaa, E. Z. (2017). Silver nanoparticles as an antimicrobial agent: A case study on *Staphylococcus aureus* and *Escherichia coli* as models for Gram-positive and Gram-negative bacteria. J Gen Appl Microbiol, 63(1), 36-43.

Gurunathan S, Han JW, Kwon DN, Kim JH (2014) Enhanced antibacterial and anti-biofilm activities of silver nanoparticles against Gram-negative and Gram-positive bacteria. Nanoscale Res Lett 9: 373-388. https://www.jstage.jst.go.jp/article/jgam/63/1/63_2016.07.004/_article/-char/ja/

Gurunathan, S., Han, J. W., Park, J. H., Kim, E., Choi, Y. J., Kwon, D. N., and Kim, J. H. (2015). Reduced graphene oxide–silver nanoparticle nanocomposite: a potential anticancer nanotherapy. Int J Nanomedicine, 10, 6257. https://dx.doi.org/10.2147%2FIJN.S92449

Hanaor, D., Michelazzi, M., Leonelli, C., and Sorrell, C. C. (2012). The effects of carboxylic acids on the aqueous dispersion and electrophoretic deposition of ZrO2. J Eur Ceram, 32(1), 235-244. https://doi.org/10.1016/j.jeurceramsoc.2011.08.015

Hassoun, A., Aït-Kaddour, A., Abu-Mahfouz, A. M., Rathod, N. B., Bader, F., Barba, F. J., ... & Regenstein, J. (2022). The fourth industrial revolution in the food industry-Part I: Industry 4.0 technologies. Critical Reviews in Food Science and Nutrition, 1-17. https://doi.org/10.1080/10408398.2022.2034735

Hazarika, S. N., Gupta, K., Shamin, K. N. A. M., Bhardwaj, P., Boruah, R., Yadav, K. K., ... and Namsa, N. D. (2016). One-pot facile green synthesis of biocidal silver nanoparticles. Mater Res Express, 3(7), 075401. https://iopscience.iop.org/article/10.1088/2053-1591/3/7/075401/meta

Jaworski, S., Wierzbicki, M., Sawosz, E., Jung, A., Gielerak, G., Biernat, J., ... and Chwalibog, A. (2018). Graphene oxide-based nanocomposites decorated with silver nanoparticles as an antibacterial agent. Nanoscale Res Lett, 13(1), 1-17. https://doi.org/10.1186/s11671-018-2533-2

Kafshgari, M. H., Voelcker, N. H., and Harding, F. J. (2015). Applications of zero-valent silicon nanostructures in biomedicine. Nanomedicine, 10(16), 2553-2571. https://doi.org/10.2217/nnm.15.91

Kakoti, B. B., Deka, K., & Kataki, M. S. (2022). Role of Eco-friendly Nanotechnology for Green and Clean Technology. Sustainable Nanotechnology: Strategies, Products, and Applications, 237-247. https://doi.org/10.1002/9781119650294.ch14

Kalimuthu, K., Babu, R. S., Venkataraman, D., Bilal, M., and Gurunathan, S. (2008). Biosynthesis of silver nanocrystals by *Bacillus licheniformis*. Colloids Surf B, 65(1), 150-153. https://doi.org/10.1016/j.colsurfb.2008.02.018

Kaur, P. (2018). Biosynthesis of nanoparticles using eco-friendly factories and their role in plant pathogenicity: a review. Biotechnol Res Innov, 2(1), 63-73. https://doi.org/10.1016/j.biori.2018.09.003

Krishnaraj, C., Ramachandran, R., Mohan, K., and Kalaichelvan, P. T. (2012). Optimization for rapid synthesis of silver nanoparticles and its effect on phytopathogenic fungi. Spectrochim Acta A Mol Biomol Spectrosc, 93, 95-99. https://doi.org/10.1016/j.saa.2012.03.002

Kulkarni, R. R., Shaiwale, N. S., Deobagkar, D. N., and Deobagkar, D. D. (2015). Synthesis and extracellular accumulation of silver nanoparticles by employing radiation-resistant *Deinococcus radiodurans*, their characterization, and determination of bioactivity. Int J Nanomedicine, 10, 963. https://dx.doi.org/10.2147%2FIJN.S72888

Lengke, M., and Southam, G. (2006). Bioaccumulation of gold by sulfate-reducing bacteria cultured in the presence of gold (I)-thiosulfate complex. Geochim Cosmochim Acta, 70(14), 3646-3661. https://doi.org/10.1016/j.gca.2006.04.018

Li, J., and Liu, C. Y. (2010). Ag/graphene heterostructures: synthesis, characterization and optical properties. Eur J Inorg. Chem, 8, 1244–1248. https://doi.org/10.1002/ejic.200901048

Mallmann, E. J. J., Cunha, F. A., Castro, B. N., Maciel, A. M., Menezes, E. A., and Fechine, P. B. A. (2015). Antifungal activity of silver nanoparticles obtained by green synthesis. Rev Inst Med Trop Sao Paulo, 57, 165-167. https://doi.org/10.1590/s0036-46652015000200011

Mishra, S., Singh, B. R., Singh, A., Keswani, C., Naqvi, A. H., and Singh, H. B. (2014). Biofabricated silver nanoparticles act as a strong fungicide against *Bipolaris sorokiniana* causing spot blotch disease in wheat. Plos one, 9(5), e97881. https://doi.org/10.1371/journal.pone.0097881

Mokhtari, N., Daneshpajouh, S., Seyedbagheri, S., Atashdehghan, R., Abdi, K., Sarkar, S., ... and Shahverdi, A. R. (2009). Biological synthesis of very small silver nanoparticles by culture supernatant of *Klebsiella pneumonia*: The effects of visible-light irradiation and the liquid mixing process. Mater Res Bull, 44(6), 1415-1421. https://doi.org/10.1016/j.materresbull.2008.11.021

Morais, M. G. D., Martins, V. G., Steffens, D., Pranke, P., and da Costa, J. A. V. (2014). Biological applications of nanobiotechnology. J Nanosci Nanotechnol, 14(1), 1007-1017. https://doi.org/10.1166/jnn.2014.8748

Nam, K. T., Lee, Y. J., Krauland, E. M., Kottmann, S. T., and Belcher, A. M. (2008). Peptide-mediated reduction of silver ions on engineered biological scaffolds. ACS Nano, 2(7), 1480-1486. https://doi.org/10.1021/nn800018n

Nguyen, N. T. T., Nguyen, L. M., Nguyen, T. T. T., Nguyen, T. T., Nguyen, D. T. C., & Tran, T. V. (2022). Formation, antimicrobial activity, and biomedical performance of plant-based nanoparticles: a review. Environmental Chemistry Letters, 1-41. https://doi.org/10.1007/s10311-022-01425-w

O'connor, B. P. (2000). SPSS and SAS programs for determining the number of components using parallel analysis and Velicer's MAP test. Behav. res. meth. Instrum., 32(3), 396-402. https://doi.org/10.3758/BF03200807

Okumura, A., Saito, K., and Tatsuma, T. (2016). Asymmetric optical properties of photocatalytically deposited plasmonic silver nanoparticles. Phys Chem Chem Phys, 18(10), 7007-7010. https://doi.org/10.1039/C6CP00331A

Panter, F., Popoff, A., Garcia, R., Krug, D., & Müller, R. (2022). Myxobacteria of the Cystobacterineae suborder are producers of new vitamin K_2 derived myxoquinones. Microorganisms, 10(3), 534. https://doi.org/10.3390/microorganisms10030534

Quiroga, E. N., Sampietro, A. R., and Vattuone, M. A. (2004). *In vitro* fungitoxic activity of *Larrea divaricata* cav. extracts. Lett Appl Microbiol, 39(1), 7-12. https://doi.org/10.1111/j.1472-765X.2004.01521.x

Radzig, M. A., Nadtochenko, V. A., Koksharova, O. A., Kiwi, J., Lipasova, V. A., and Khmel, I. A. (2013). Antibacterial effects of silver nanoparticles on gram-negative bacteria: influence on the growth and biofilms formation, mechanisms of action. Colloids Surf B, 102, 300-306. https://doi.org/10.1016/j.colsurfb.2012.07.039

Rathod, V., Banu, A., and Ranganath, E. (2012). Biosynthesis of highly stabilized silver nanoparticles by Rhizopus stolonifer and their anti-fungal efficacy. Int J Curr Pharm Res, 2(1), 241-245. https://www.sid.ir/en/journal/ViewPaper.aspx?ID=227254

Ruud, C. O., Barrett, C. S., Russell, P. A., and Clark, R. L. (1976). Selected area electron diffraction and energy dispersive X-ray analysis for the identification of asbestos fibres, a comparison. Micron (1969), 7(2), 115-132. https://doi.org/10.1016/0047-7206(76)90055-8

Sathishkumar, M., Sneha, K., and Yun, Y. S. (2010). Immobilization of silver nanoparticles synthesized using *Curcuma longa* tuber powder and extract on cotton cloth for bactericidal activity. Bioresour Technol, 101(20), 7958-7965. https://doi.org/10.1016/j.biortech.2010.05.051

Shahverdi, A. R., Minaeian, S., Shahverdi, H. R., Jamalifar, H., and Nohi, A. A. (2007). Rapid synthesis of silver nanoparticles using culture supernatants of Enterobacteria: a novel biological approach. Process Biochem, 42(5), 919-923. https://doi.org/10.1016/j.procbio.2007.02.005

Sharma, P., Teixeira de Mattos, M. J., Hellingwerf, K. J., and Bekker, M. (2012). On the function of the various quinone species in Escherichia coli. The FEBS journal, 279(18), 3364-3373. https://doi.org/10.1111/j.1742-4658.2012.08608.x

Sintubin, L., De Windt, W., Dick, J., Mast, J., Van Der Ha, D., Verstraete, W., and Boon, N. (2009). Lactic acid bacteria as reducing and capping agent for the fast and efficient production of silver nanoparticles. Appl Microbiol Biotechnol, 84(4), 741-749. https://doi.org/10.1007/s00253-009-2032-6

Sugimoto, S., Higashi, C., Matsumoto, S. and Sonomoto, K. (2010). Improvement of multiple-stress tolerance and lactic acid production in *Lactococcus lactis* NZ9000 under conditions of thermal stress by heterologous expression of *Escherichia coli* dnaK. Appl Environ Microbiol 76(13): 4277-4285. https://doi.org/10.1128/AEM.02878-09

Thenmozhi, M., Kannabiran, K., Kumar, R., and Khanna, V. G. (2013). Antifungal activity of *Streptomyces* sp. VITSTK7 and its synthesized Ag_2O/Ag nanoparticles against medically important *Aspergillus* pathogens. JMM, 23(2), 97-103. https://doi.org/10.1016/j.mycmed.2013.04.005

Vahdati, A. R., and Sadeghi, B. (2013). A study on the assessment of DNA strand-breaking activity by silver and silica nanoparticles. J Nanostructure, 3(1), 1-3. https://doi.org/10.1186/2193-8865-3-7

Vandana S, and Archana T (2016) Combating pathogenic microbes through *E. coli*-based silver nano tools. IJPBS 7: 367-375.

Wang, Z. L. (2000). Transmission electron microscopy of shape-controlled nanocrystals and their assemblies. J Phys Chem, 104(6), 1153-1175. https://doi.org/10.1021/jp993593c

Yoshida, A., & Freese, E. (1975). Lactate dehydrogenase from *Bacillus subtilis*. In Methods in enzymology (Vol. 41, pp. 304-309). Academic Press. https://doi.org/10.1016/S0076-6879(75)41069-2

Zheng, L., Xiong, L., Li, Y., Xu, J., Kang, X., Zou, Z., ... and Xia, J. (2013). Facile preparation of polydopamine-reduced graphene oxide nanocomposite and its electrochemical application in simultaneous determination of hydroquinone and catechol. Sens Actuators B Chem, 177, 344-349. https://doi.org/10.1016/j.snb.2012.11.006